THE JOURNAL OF PHYSICAL CHEMISTRY B

Article

pubs.acs.org/JPCB

Interaction and Dynamics of Associated Formamide in TX100–Formamide Binary Mixtures by Dielectric Spectroscopy

Juan Wang and Kongshuang Zhao*

College of Chemistry, Beijing Normal University, 100875 Beijing, China

Supporting Information

ABSTRACT: Dielectric behaviors of a binary mixture composed of TX100 (a nonionic surfactant) and formamide (FA) at different surfactant concentrations and varying temperature were investigated over a frequency range from 40 Hz to 110 MHz. One relaxation appeared around gigahertz is considered to be from the contribution of two types of FA; one is "free FA", which has no interaction with surfactant, and the other is "associated FA", which can interact with surfactant. Conductivity was used to determine the number of associated FAs, and the result indicates that each ethylene oxide (EO) segment binds to one FA molecule. The dipole moment of the associated FA was calculated by using Cavell equation, and it is smaller than those of bulk FA, while the dipole rotation time of associated FA is higher than that of bulk FA. This suggests that the dynamics of associated FA is restricted by the hydrophilic chain of surfactant. The thermodynamic parameters, obtained from the temperature dependences of the relaxation times, revealed that in dilute TX100–FA solution the interaction of FA with EO segment of surfactant is weaker compared with the FA–FA hydrogen bond. This work also demonstrated that the dynamics of associated FA is quite similar to that of hydration water.

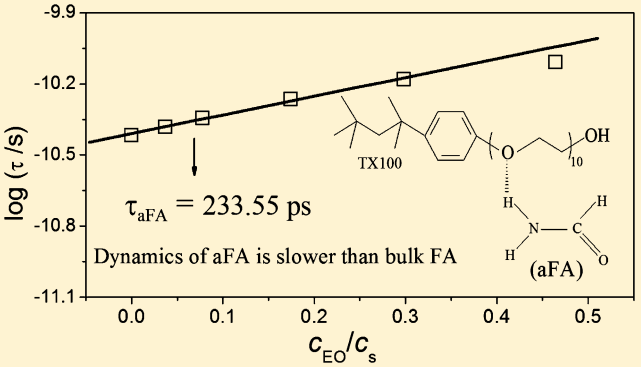

1. INTRODUCTION

Formamide (FA) is the most common studied solvent in surfactant nonaqueous systems because it has some similar physical properties with water, such as high polarity, high structure, and sufficient cohesive force. These properties ensure that the surfactant can form aggregation in FA and have focused much research[1−7] on the micellization behaviors of surfactant in FA by various techniques, such as surface tension measurements,[3,4] NMR,[5] and light scattering technology.[6,7] The data obtained by these methods include ionic surfactant (e.g., CTAB and SDS[3]) and nonionic surfactant (e.g., Triton X-100 (TX100),[4] CxEy,[5] and PEO-PPO-PEO[6,7]). Undoubtedly, this research revealed the important micellization behaviors (e.g., cmc, aggregation number, and free energy of micellization) of these surfactants in FA. However, most of these studies are from point of view of properties of micelles, while several issues regarding the properties of FA in surfactant–FA systems remain still unclear.

The first question is about the dynamic properties of FA molecule that is associated with the surfactants. For surfactant aqueous, there are at least two types of water:[8] the hydration water that interacts with the surfactant and the free water that has no interaction with the surfactant. The structure and dynamics of hydration water in surfactant systems have been studied by a variety of different ways,[9,10] such as FTIR,[11] fluorescence,[12] and NMR.[13] Similarly, in the systems composed of surfactant and FA, there also exist two types of FA: associated FA and free FA. However, comparing with the studies about the properties of the hydration water, the reported information about the nature of interaction and the dynamics of the associated FA in surfactant systems is limited.[14−16]

A second question is about the similarity between FA and water. From the point view of micellization, although there are quantitative differences, the general behavior of surfactant in FA is qualitatively similar to the corresponding aqueous systems. Therefore, FA is a water-like solvent and can be used as water substitute in surfactant systems.[17] However, it is necessary to make a deeper analysis about the properties of associated FA and hydration water to understand the similarity between FA and water.

Dielectric relaxation spectroscopy (DRS) is sensitive to the polarization processes related to molecular-level dipoles. Thus, it has advantages on studying micellar systems and dynamics of solvents such as hydration water.[10,18−24] For example, Asami[20] measured the dielectric spectroscopy of TX100–water binary mixtures and calculated the number of hydration waters per ethylene oxide (EO) segment by means of conductivity. Buchner et al. studied the relaxation and cooperative dynamics of hydration water in both ionic[21] and nonionic[22] surfactant

Received: January 22, 2013
Revised: May 18, 2013
Published: May 21, 2013

dx.doi.org/10.1021/jp400762s | J. Phys. Chem. B 2013, 117, 7026−7033

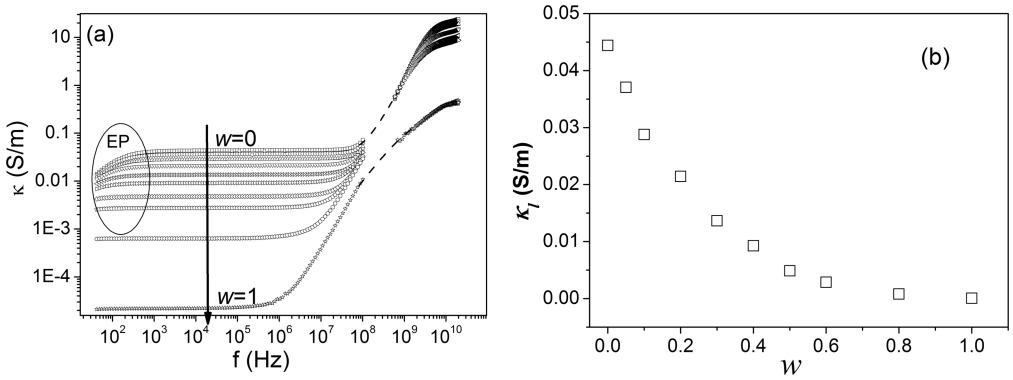

Figure 1. (a) Frequency dependences of conductivity of TX100−FA mixtures with different weight fraction of TX100. The coordinate axes are logarithmic. (b) Dependence of weight fraction of TX100 on low-frequency conductivity κ_l of TX100−FA mixtures. Data were obtained at 5 MHz.

systems. However, studies on the associated FA in surfactant systems by DRS are rare.

To answer the two questions previously mentioned, we have conducted studies on TX100−formamide binary mixtures by DRS. TX100 is a nonionic surfactant having 10 EO segments in its hydrophilic chain and can form micelles in FA.[4] In the palisade layer of the micelle, FA can associate with EO segments. The main aim of this work is to discuss the properties of the associated FA, including its associated numbers, dipole moment, and relaxation time. Through the comparison with properties of hydration water in TX100−water mixtures, the similarity of FA and water are further discussed.

2. MATERIALS AND METHODS

2.1. Materials. Triton X-100 (*p*-(1,1,3,3-tetramethylbutyl)-phenoxypolyoxyethyleneglycol) (TX100) used in this work was purchased from Amresco Chemical. FA was analytical grade and obtained from Beijing Chemical Works, China. A series of binary mixtures was prepared by dissolving TX100 in FA and double-distilled water, respectively. The weight fraction of TX100, *w*, was in the range of 0−100%. These binary mixtures were subjected to dielectric measurements.

2.2. Dielectric Measurements. The dielectric measurements of the binary mixtures were accomplished by two instruments. The low-frequency measurements (40 Hz to 110 MHz) were carried out with a HP 4294A Precision Impedance Analyzer (from Agilent Technologies), which is controlled by a personal computer. The amplitude of the applied alternating field was 500 mV, and a measurement cell with concentrically cylindrical platinum electrodes was employed.[25] The cell constant C_l, stray capacitance C_r, and residual inductance L_r that have been determined by the use of several standard substances (air, pure ethanol, and pure water) were 0.072 pF, −0.716 pF, and 5.23×10^{-8} (F/S^2), respectively. The experimental data errors arising from the residual inductance and measurement cell were corrected by Schwan method.[26] Then, the corrected data of capacitance C_s and conductance G_s at each frequency were converted to permittivity and conductivity using the following equations: $\varepsilon = C_s/C_l$ and $\kappa = G_s\varepsilon_0/C_l$ (ε_0 (= 8.8541×10^{-12} F/m) is the vacuum permittivity). The low-frequency limit of conductivity, κ_l, can be read directly from the low-frequency plateau in the $\kappa \sim f$ plot. The high-frequency dielectric measurements (100 MHz to 20 GHz) were carried out with an Agilent E8362B PNA Series Network Analyzer (Agilent Technologies), which equipped with an Agilent 85070E open-ended coaxial probe. By means of built-in software of this measuring system, permittivity and total dielectric loss were automatically calculated as a function of measuring frequency. All measurements were maintained at 22.8 ± 0.1 °C. For the samples with $w = 0.05$, high-frequency measurements were also carried out at a series of temperature ranges from 25.8 to 45.3 °C.

3. RESULTS AND DISCUSSION

3.1. Conductivity and the Number of Associated FAs per EO Segment in TX100−FA Binary Mixtures. The dc conductivity obtained from DRS has been efficiently used to calculate the number of hydration water[20,27] and other associating solvent[28,29] in surfactant systems. To calculate the number of associated FAs in TX100−FA mixtures, dc conductivity of TX100−FA mixtures should be determined first. In this work, TX100−FA mixtures show distinct dielectric relaxation at high frequency (~8 GHz, as shown in Figures 1a and 5.) Thus, conductivity at low frequencies far below the dielectric relaxation can be treated as dc conductivity. In the low-frequency range, conductivity would be influenced by EP effect (as shown in Figure 1a), the conductivity sharply decrease with decrease in frequency in the very low frequency range.[30] In the frequency range of $10^4 \sim 10^7$ Hz, the conductivity is almost independent of measuring frequency for all concentrations. Therefore, to avoid the EP effect as far as possible, the low-frequency conductivity κ_l of the systems was read at 5 MHz and is plotted in Figure 1b. It is clear that the value of the conductivity κ_l is a nonlinear decreasing function of TX100 concentrations.

When the TX100 forms a spherical micelle in FA, the TX100−FA binary solution can be modeled as a suspension, that is, the micelles with conductivity κ_p dispersed in a continuous FA medium with conductivity κ_a in volume fraction ϕ. The suspension has conductivity κ_l. According to Bruggeman's mixture theories, the conductivity κ_l is given by:[20,31]

$$\left(\frac{\kappa_l - \kappa_p}{\kappa_a - \kappa_p}\right)\left(\frac{\kappa_a}{\kappa_l}\right)^{1/3} = 1 - \phi \quad (1)$$

Bruggeman's equation was obtained by considering a regular distribution of spherical equivalent objects. When the regular distribution is not realistic, the use of Looyenga equation could have been better:[20,32]

$$\kappa_l^{1/3} = (1 - \phi)\kappa_a^{1/3} + \phi\kappa_p^{1/3} \quad (2)$$

dx.doi.org/10.1021/jp400762s | J. Phys. Chem. B 2013, 117, 7026−7033

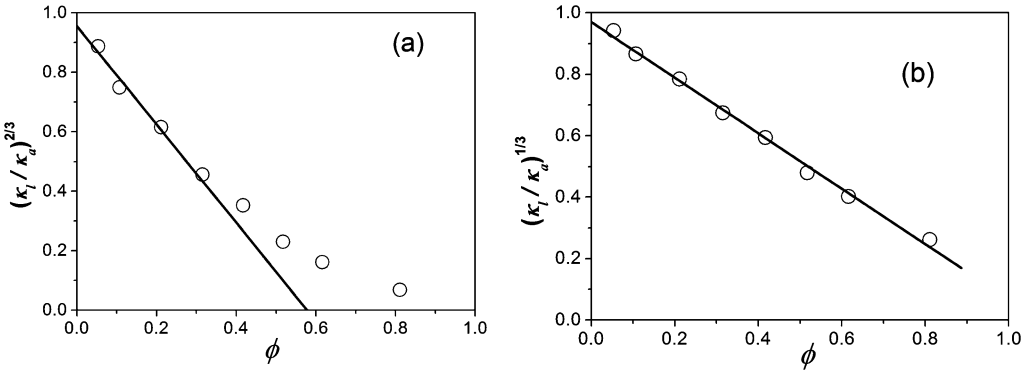

Figure 2. Plot of the conductivity ratios (a) $(\kappa_l/\kappa_a)^{2/3}$ and (b) $(\kappa_l/\kappa_a)^{1/3}$ versus volume fraction ϕ of micelles. The solid line is the best fit to eqs 5 and 6, respectively.

It should be noticed that when TX100 is added to FA it remains in the form of monomers until the critical micelle concentration (cmc) is reached. Therefore, the continuous medium is actually a mixture that is combined with FA and TX100 monomers rather than pure FA. However, considering that the cmc of TX100 in FA is low (~100 mmol/kg[4]), the conductivity of continuous medium κ_a is approximate to the conductivity of pure FA. Because both the conductivity κ_l of TX100−FA solution and the conductivity κ_a of FA are much larger than those of TX100 (micelles), that is, κ_l, $\kappa_a \gg \kappa_p$, eqs 1 and 2 can be, respectively, simplified as:

$$(\kappa_l/\kappa_a)^{2/3} = 1 - \phi \tag{3}$$

and

$$(\kappa_l/\kappa_a)^{1/3} = 1 - \phi \tag{4}$$

The TX100 micelle can be considered to be a sphere with a palisade layer made of the hydrophilic chains of TX100 molecule around the inner spherical hydrophobic head. FA molecule can permeate into the palisade layer and interact with the EO segment in the hydrophilic chain. Compared with bare micelle (which no FA permeated into), the volume fraction of the actual micelle (which FA permeated into) will become $\alpha\phi$. Thus, eqs 3 and 4 can be represented by:

$$(\kappa_l/\kappa_a)^{2/3} = 1 - \alpha\phi \tag{5}$$

and

$$(\kappa_l/\kappa_a)^{1/3} = 1 - \alpha\phi \tag{6}$$

where α (= V_b/V_a) is the volume ration of the actual micelle, V_b, to the bare micelle, V_a. From eqs 5 and 6, we obtained the values of α by fitting the result shown in Figure 2, which is from the data of Figure 1b. In Figure 2, ϕ is converted from concentrations of TX100 (w) by taking the volume of TX100 as 0.946 $cm^3\ g^{-1}$ (calculated from the density measurement described in the Supporting Information). The obtained values of α are 1.652 for eq 5 and 0.903 for eq 6.

Because the values of V_b and V_a are both proportional to the aggregation number, α is equivalent to the volume ration between a solvated single monomer and the relative bare volume:

$$\alpha = (V_{TX} + 10n_{aFA}V_{FA})/V_{TX} \tag{7}$$

where n_{aFA} is the associated number of FAs per EO segment and 10 is the number of EO segments in the TX100 hydrophilic chain. V_{TX} and V_{FA} are the volumes of TX100 and FA, respectively. Therefore, the quantity α-1 is expressed as the volume ratio of associated FA to TX100:

$$\alpha - 1 = \frac{10n_{aFA}V_{FA}}{V_{TX}} = \frac{\upsilon_{FA}}{\upsilon_{TX}}\frac{c_{aFA}M_{FA}}{c_{TX}M_{TX}} \tag{8}$$

where c, υ, and M are molar concentration, specific partial volume, and molecular weight, respectively. The subscripts FA, aFA, and TX denote the free FA, associated FA, and TX100, respectively. As such, the associated number n_{aFA} per EO segment was calculated by the following equation using M_{TX} = 646.85, υ_{TX} = 0.946 $cm^3\ g^{-1}$, M_{FA} = 45.04, and υ_{FA} = 0.882 $cm^3\ g^{-1}$:

$$n_{aFA} = \frac{c_{aFA}}{10c_{TX}} = (\alpha - 1)\frac{\upsilon_{TX}M_{TX}}{10\upsilon_{FA}M_{FA}} \tag{9}$$

The number n_{aFA} determined using Bruggeman's equation is 1.004. This means that every EO segment in TX100 molecule bound with one FA molecules. For the microscopic mechanism of the interaction between TX100 and FA, it may be explained as follows: Because in EO segment the oxygen atom has two pairs of unpaired electron, each EO segment can combine with two FA molecules at least. However, steric effect should be considered. From the resonance structure of FA[33,34] shown in Figure 3, it can be seen that in FA molecule there is a double

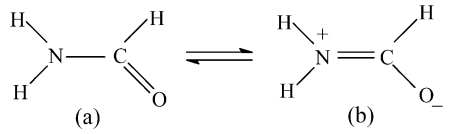

Figure 3. Resonance structure of FA molecule.

bond that can transform between the N−C and C−O bonds. Therefore, N−C bond cannot freely rotate due to its partial double-bond character,[33] that is, the molecule of FA is planar. This planar structure increases the rigidity and steric effect of FA molecule and restricts the associated number to EO segments.

The number n_{aFA} determined using Looyenga's equation is −0.15. This negative value is unreasonable. It means that for TX100−FA systems Bruggeman's equation is more available than Looyenga's equation. On the basis of Bruggeman's equation, a linear relation between $(\kappa_l/\kappa_a)^{2/3}$ and ϕ is found at ϕ < 0.4 in Figure 2a, indicating that regular spherical micelles are formed below this concentration range.

dx.doi.org/10.1021/jp400762s | J. Phys. Chem. B 2013, 117, 7026−7033

The number of associated FA to EO segments can also be obtained by other experimental techniques; for example, in the work of Alexandridis,[6] the associated number of FAs obtained by using small-angle neutron scattering is ~1.5. This result is close to ours. Moreover, from many studies on the polymer (which has EO segments)−water systems,[20,22,35,36] it was concluded that two to five water molecules bonded to each EO segment. Compared with the number of hydration waters to EO segment, the number of associated FA molecules is smaller. In our previous work, the number of associated ionic liquid (ILs) per EO segments in TX100-IL systems have been calculated;[28,29] the results showed that the associated number of hydrophilic ILs and hydrophobic ILs to EO segment is 0.85 and 1.09, respectively. It seems that the associated number of organic solvents to the EO segment is smaller than that of hydration water. The difference of associated number between organic solvent and water may be relevant to the steric effect and the bonding ability of organic solvents.

Although FA can also form a hydrogen bond with EO segments in the TX100−FA binary mixture, the interaction between FA and EO segments is more complex than that of water and EO segments due to the resonance structure of FA molecule. From Figure 3, it is clear that the FA molecule has two atoms that can form a hydrogen bond to the EO segment of TX100 molecule: one is the hydrogen of $-NH_2$ in resonance structure (a) and another is the electropositive nitrogen in resonance structure (b). Thus, there are at least two association modes between TX100 and FA, as shown in Figure 4. Regardless of what kind of mode, the dipole moment and dynamics of associated FA will be affected by EO segments, and they will be discussed in detail in the next section.

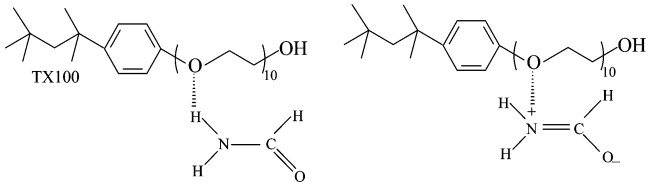

Figure 4. Chemical structures of interaction between TX100 and FA.

3.2. Dipole Moment and Dynamics of Associated FA.

3.2.1. Dielectric Spectra of Binary Mixtures. We have modeled the micellar systems as heterogeneous particle suspensions and interpreted the data of conductivity based on Bruggeman mixture theories. Heterogeneous systems always exhibit interfacial polarization relaxation in the low-frequency range. However, in some special heterogeneous systems, this relaxation is undetectable because its strength is determined by conductivity and permittivity of constitute phase.[37] For systems studied in this work, neither TX100−FA nor TX100−water shows distinct relaxation in the low-frequency range. (Data are not shown.) Thus, we cannot gain more information about the whole micelle from low-frequency data. However, we can focus on the properties of associated FA in the palisade layer of micelle based on high-frequency measurements because high-frequency relaxations are mainly relative to dipolar polarization of solvent.

The high-frequency dielectric spectra of (a) TX100−FA and (b) TX100−water binary mixtures at all measured concentrations are displayed in Figure 5. From Figure 5, it is clear that the dielectric relaxations of TX100−FA and TX100−water systems occur at about 5 and 10 GHz, respectively. For polymer−solvent systems, the contributions to the high process of dielectric relaxation may mainly include two parts: solvent and polymer segment. However, the contribution of polymer segment (such as EO segment) is always smaller than that of pure solvent.[38,39] In some systems, the contribution of polymer segment can be ignored during dielectric analysis. For example, in the studies of Kaatze et al.,[8] which focused on the dielectric relaxations of aqueous solutions of oxygen-containing hydrocarbon polymers at 0.4−40 GHz, the contribution of EO segment in dilute solution is ignored because its relaxation strength is too small. Besides, in the research reported by other groups, for example, Asami,[20] Buchner et al.,[22] Borodin et al.,[40] and Shinyashiki et al.,[41] the similar treatment, that is, neglecting the contribution of polymer segment, is also available. In this work, although dielectric relaxation caused by EO segment can also be observed in pure TX100 below 5 GHz, the relaxation strength and dielectric loss of EO segment are significantly smaller that those of pure solvent (as shown in Figure 5, $w = 0$ and 1). Considering that the concentrations of TX100 studied are relatively low, the contribution of EO segment is negligible in this frequency range. Therefore, in our work, the observed high-frequency relaxations in TX100−FA and TX100−water systems are attributed to FA and water relaxation, respectively.

To examine the dielectric spectra in detail and obtain more information on the inner structure and dynamics of the two systems, we obtained the dielectric parameters characterizing the dielectric behaviors of the systems by fitting the following Cole−Cole equation[42] to the experimental data:

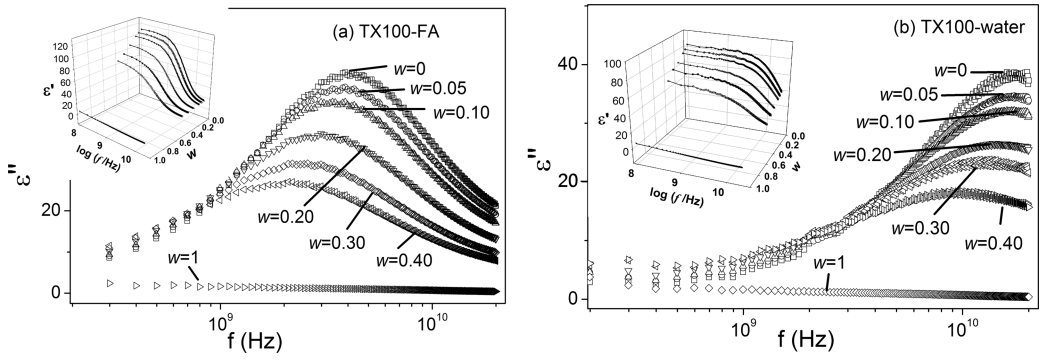

Figure 5. Dielectric loss, ε'', ascribing to dielectric relaxation as a function of frequency for the binary mixtures: (a) TX100−FA and (b) TX100−water with different TX100 mass fraction. The inset shows the corresponding 3D plot of permittivity ε' as a function of frequency and TX100 mass fraction.

dx.doi.org/10.1021/jp400762s | J. Phys. Chem. B 2013, 117, 7026−7033

$$\varepsilon* = \varepsilon' - j\varepsilon'' = \varepsilon_h + \frac{\Delta\varepsilon}{1 + (j\omega\tau)^{\beta}} \quad (10)$$

where $\Delta\varepsilon = \varepsilon_l - \varepsilon_h$ (ε_l, and ε_h are the low- and high-frequency limits of permittivity, respectively) and τ ($\tau = 1/2\pi f_0$, f_0 is characteristic relaxation frequency) indicates relaxation strength (or dielectric increment) and relaxation time, respectively. β is the Cole–Cole parameter ($0 < \beta \leq 1$), indicating the distribution of relaxation times. All of the dielectric spectra were well-represented by eq 10 with the best fitting. The parameters obtained from Figure 5 are listed in Table 1.

Table 1. Dielectric Parameters for TX100–FA and TX100–Water Systems (22.8 °C)

TX100–FA				
w	ε_l	$\Delta\varepsilon$	τ (ps)	β
0	114.45	106.57	38.35	1.00
0.05	106.55	100.59	41.60	0.96
0.10	100.74	94.97	45.31	0.90
0.20	89.82	84.53	54.39	0.88
0.30	77.61	72.92	66.03	0.82
0.40	69.15	64.12	78.87	0.78
TX100–water				
w	ε_l	$\Delta\varepsilon$	τ (ps)	β
0	81.20	77.80	9.04	1.00
0.05	77.22	70.76	9.63	0.99
0.10	73.92	67.33	10.19	0.95
0.20	65.52	59.03	11.74	0.90
0.30	60.58	54.17	13.79	0.88
0.40	50.96	44.61	18.70	0.80

From Table 1, it can be seen that the parameters β decrease with increasing TX100 concentrations, indicating that the observed relaxation is not attributed to one mechanism. For the TX100–FA mixture, there are two types of FA molecule, as previously mentioned, the "free FA" and the "associated FA". The observed dielectric spectra in Figure 5a can be considered to be from the superimposed result of the contribution of the two types of FA. Similarly, the dielectric spectra in Figure 5b were caused by the hydration water and free water.

3.2.2. Dipole Moment of Associated FA. Cavell equation[22,43] is a quantitative formula describing the relation between the dielectric increment $\Delta\varepsilon$ and the effective dipole moment μ of the species responsible for a relaxation process:

$$\frac{2\varepsilon_l + 1}{\varepsilon_l}\Delta\varepsilon = \frac{N_A c}{k_B T\varepsilon_0}\mu^2 \quad (11)$$

where c, N_A, k_B, and T are molar concentration, Avogadro constant, Boltzmann constant, and absolute temperature, respectively. For "associated FA" and "free FA" molecule, there are:

$$\frac{2\varepsilon_l + 1}{\varepsilon_l}\Delta\varepsilon_1 = \frac{N_A c_{aFA}}{k_B T\varepsilon_0}\mu_1^2 \quad (12)$$

$$\frac{2\varepsilon_l + 1}{\varepsilon_l}\Delta\varepsilon_2 = \frac{N_A c_{FA}}{k_B T\varepsilon_0}\mu_2^2 \quad (13)$$

where μ_1 and μ_2 are the dipole moments of associated FA and free FA, respectively. $\Delta\varepsilon_1$ and $\Delta\varepsilon_2$ are dielectric increments that are caused by associated FA and free FA, respectively.

Because the concentration of TX100 is relatively low and in the investigated high-frequency range TX100 is not contributing (Figure 5), the observed dielectric increment $\Delta\varepsilon$ can be just treated as a linear superposition by two types of FA, that is, $\Delta\varepsilon = \Delta\varepsilon_1 + \Delta\varepsilon_2$. Therefore, combined with eqs 12 and 13, we get the formula:

$$\frac{2\varepsilon_l + 1}{\varepsilon_l}\Delta\varepsilon = \frac{N_A}{k_B T\varepsilon_0}(c_{aFA}\mu_1^2 + c_{FA}\mu_2^2) \quad (14)$$

After dividing the total concentration of FA, c_s, on both side of eq 14, there is:

$$\frac{2\varepsilon_l + 1}{\varepsilon_l}\frac{\Delta\varepsilon}{c_s} = \frac{N_A}{k_B T\varepsilon_0}[x_{aFA}\mu_1^2 + (1 - x_{aFA})\mu_2^2] \quad (15)$$

where x_{aFA} is the molar fraction of associated FA: $x_{aFA} = n_{aFA}(c_{EO}/c_s)$. Thus, eq 15 can be rewritten as:

$$\frac{(2\varepsilon_l + 1)\Delta\varepsilon}{\varepsilon_l c_s \mu_2^2}\frac{k_B T\varepsilon_0}{N_A} - 1 = n_{aFA}(c_{EO}/c_s)(\mu_1^2/\mu_2^2 - 1) \quad (16)$$

It should be notice that eq 16 is available in dilute solutions because when TX100 concentration is high enough, the contribution of TX100 is not negligible and eq 14 would not be unacceptable.

With the relative data (ε_l,$\Delta\varepsilon$) in Table 1 and the number of associated FAs obtained in Section 3.1, the dipole moment of associated FA molecule can be calculated according to eq 16. The ratio of squared effective dipole moments of associated FA and free FA $(\mu_1^2/\mu_2^2)_{FA}$ are plotted as a function of TX100 concentration in Figure 6. Meanwhile, for the sake of comparison, the dipole moment of hydration water is also calculated in the same way, and the ratio for water $(\mu_1^2/\mu_2^2)_{water}$ is also plotted in Figure 6.

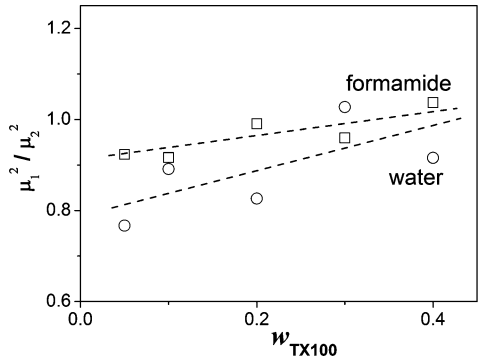

Figure 6. Dependence of TX100 concentration on the ratio of squared effective dipole moments of associated solvent and free solvent, μ_1^2/μ_2^2, for TX100–FA (□) and TX100–water (○). The dashed lines are just guides to the eyes rather than indicate that the plot is a linear function of TX100 concentrations.

The following limits have to be fulfilled: At $w = 0 \Rightarrow \mu_1^2/\mu_2^2 = 1$ because in this case there is just pure solvent. The difference between associated FA and free (or bulk) FA can be made out in Figure 6. As can be seen in Figure 6, the values of $(\mu_1^2/\mu_2^2)_{FA} \leq 1$, indicating that the EO segment has a negative effect on dipole moment of associated FA; that is, the interaction of EO segment can decrease the polarity of associated FA. This may be interpreted as follows: in bulk FA, the electronegative atom that forms the hydrogen bond is O in the –CHO group,

dx.doi.org/10.1021/jp400762s | J. Phys. Chem. B 2013, 117, 7026–7033

whereas in TX100−FA mixtures, the electronegative atom is O in EO segment. Compared with O in the −CHO group, the electronegativity of O in the EO segment is smaller, which may decrease the effective polarity of associated FA. Also, the dipole moment of associated FA is related to surfactant concentrations, and this may due to the change of microenvironment around associated FA. Here the microenvironment mainly refers to the structure of EO chain in the palisade layer of micelles. Because the aggregation number of TX100 is increased when TX100 concentrations increase,[4] this suggests that the structure of the EO chain in the palisade layer changes from a looser structure to a tighter structure. The tighter structure of EO chain can influence the interaction between EO and associated FA, which affects the dipole moment of associated FA. The above discussions are focused on a dilute solution where the contributions of EO segment are ignored. Indeed, in systems in which the contribution of EO segment must be considered, the relaxation of associated FA or water molecules can be included in the lower frequency process with surfactant molecules.[35] However, in this case, the dipole moment of associated solvent cannot be calculated by using eq 16 any more.

The similarity between FA and water can also be shown in Figure 6 to some extent. We can see that the dipole moment of hydration water is also reduced (compared with bulk water) and also related to surfactant concentrations, which is similar to associated FA.

3.2.3. Relaxation Time of Associated FA. The logarithm of the relaxation time observed can be considered to be a linear function of x_{aFA}:[20,44]

$$\log \tau = (1 - x_{aFA}) \log \tau_2 + x_{aFA} \log \tau_1 \quad (17)$$

where τ_1 and τ_2 are the relaxation time of associated FA and free FA, respectively. Because x_{aFA} is given by $x_{aFA} = n_{aFA}(c_{EO}/c_s)$, eq 14 can be represented as:

$$\log \tau = \log \tau_2 + n_{aFA}(c_{EO}/c_s) \log(\tau_1/\tau_2) \quad (18)$$

Using eq 18, the logarithm of the relaxation time in Table 1, log τ, was plotted as a function of (c_{EO}/c_s) in Figure 7. It can be seen from Figure 7 that there is a linear relationship between log τ and (c_{EO}/c_s) and the slope provides the value of n_{aFA} $\log(\tau_1/\tau_2)$. With the associated number obtained in Section 3.1, the values of τ_1/τ_2 and τ_1 for associated FA were calculated and listed in Table 2. Meanwhile, for the sake of comparison, the relaxation time of hydration water in TX100−water mixtures was calculated with the same method (also plotted in Figure 7) and listed in Table 2.

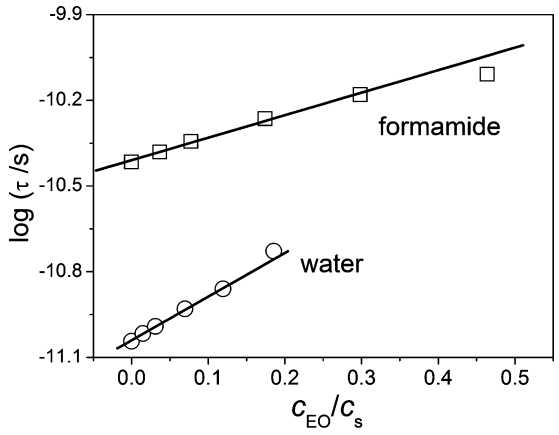

Figure 7. Dependence of molar ration of EO segment to solvent, c_{EO}/c_s, on the logarithm of the relaxation time, log τ. The solid line is the best fit to eq 18.

Table 2. Relaxation Time and of Free and Associated Solvent Calculated from the Linear Regression Lines Shown in Figure 7 Using Equation 18

	τ_1/τ_2	τ_2 (ps)	τ_1 (ps)
TX100−FA	6.09	38.35	233.55
TX100−water	4.08	9.04	36.88

From Table 2, it can be seen that in TX100−water binary mixtures, the dipole rotation time of hydration water, $(\tau_1)_{water}$, is longer than that of bulk water, $(\tau_2)_{water}$. This result is coinciding with the studies on the dynamics of water in organized systems, which have shown that the dynamics of hydration water is slower than that of bulk water.[10] It should be noted that in TX100−FA binary mixtures the dipole rotation time of associated FA, $(\tau_1)_{FA}$, is also longer than that of bulk FA, $(\tau_2)_{FA}$, suggesting that the dynamics of associated FA is also restricted by the hydrophilic chain of surfactant. This also shows the similarity between associated FA and hydration water.

3.2.4. Thermodynamic Parameters of Relaxation Process and Interactions between Associated FA and Surfactants. As is well known, increasing temperature can accelerate thermal motion of molecules and change the viscosity of solvent, which can further result in the weakening of hydrogen bonding between solvents and surfactants. Therefore, temperature becomes one of the important thermodynamic parameters to investigate the dynamic behavior of solvents in surfactant systems. To evaluate how the temperature affects the dynamics behavior of associated FA, we used the Eyring equation[45] to express the relationship between relaxation time and temperature.

$$\ln \tau = \ln\left(\frac{h}{kT}\right) - \frac{\Delta S}{R} + \frac{\Delta H}{RT} \quad (19)$$

where h is the Planck's constant and ΔH and ΔS are the activation enthalpy and activation entropy, respectively, of solvents. Equation 19 can be rewritten as:

$$\ln \tau T = \ln\left(\frac{h}{k}\right) - \frac{\Delta S}{R} + \frac{\Delta H}{RT} \quad (20)$$

The ln τT was plotted as a function of $1/T$ in Figure 8 for TX100−FA mixtures. From the slope and intercept of fitting line, ΔH and ΔS of FA were calculated, and the results are listed in Table 3. For comparison, ΔH and ΔS of water in TX100−water mixtures were also calculated and are listed in Table 3.

It should be noted that in both TX100−FA and TX100−water systems, there are two types of solvent molecule, that is, associated solvent and free solvent. Therefore, the activation enthalpy ΔH (or activation entropy ΔS) obtained in this work is the results of superimposition of enthalpy (or entropy) caused by the associated solvent and free solvent. This results in the observed ΔH and ΔS of solvent differing from those of pure bulk solvent (i.e., $w = 0$ in Table 3), and the difference is what the associated solvent contributed. From Table 3, it is not difficult to find that observed ΔH and ΔS in both TX100−FA

dx.doi.org/10.1021/jp400762s | J. Phys. Chem. B 2013, 117, 7026−7033

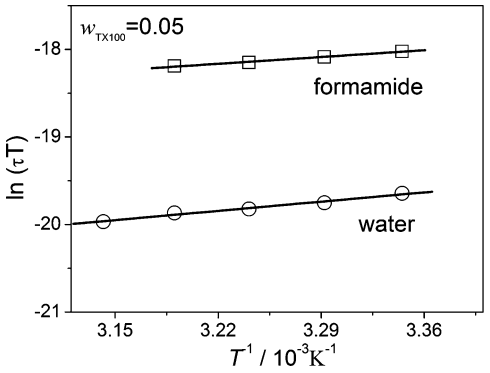

Figure 8. Natural logarithmic plot of the product of relaxation time and temperature, log τT, as a function of the inverse temperature, $1/T$, for two systems: TX100−FA (□) and TX100−water (○). The concentration of TX100 is 5 wt %. The solid line is the best fit to eq 20.

Table 3. Thermodynamics Parameters of Two Systems: TX100−FA and TX100−Water, Calculated According to Eyring Equations

	w	ΔH (kJ/mol)	ΔS (J·K^{-1}·mol^{-1})
TX100−FA	0[a]	15.90	7.4
	0.05	9.18	−16.97
TX100−water	0[a]	15.90	20.4
	0.05	12.54	7.81

[a]From ref 46. [a]From ref 47.

and TX100−water systems reduce, suggesting that in dilute TX100 solution both the associated FA and the hydration water have a slower dynamic than in the respective bulk phases. The decrease in enthalpy ΔH of associated FA (or hydration water) indicates that the interaction of FA (or water) with EO segment of surfactant is weaker compared with the hydrogen-bonding interaction between FA (or water) molecules. The decrease in entropy ΔS in TX100−FA systems indicates the decreases in degree of freedom of associated FA and this result is similar to that of hydration water. It may be further inferred that an "iceberg structure",[48] which always was employed to explain the hydrophobic effect in surfactant aqueous, also exits in surfactant−FA systems. Finally, these similarities of thermodynamics parameters suggest that the effect of interaction of EO segments on associated FA is similar to that on hydration water.

4. CONCLUSIONS

Dielectric behaviors of TX100−FA binary mixtures with varying surfactant concentrations and temperature were measured to study the interaction and dynamics of associated FA in surfactant systems. One relaxation in gigahertz was considered to be from the contribution of "free FA" and "associated FA". On the basis of Bruggeman's effective-medium approximation, the number of associated FAs was determined by conductivity. The result indicates that every EO segment associates with one FA molecule. A microexplanation about association number was given from the point view of resonance structure and steric feature of FA molecule.

The relaxation parameters, including dielectric increment and relaxation time, were obtained from fitting Cole−Cole equation to the dielectric data. By means of Cavell equation, the dipole moment of associated FA was calculated. The results indicate that in dilute TX100−FA solution the dipole moment of associated FA interacting with surfactant is lower than that of bulk FA. Moreover, combined with relaxation time and obtained associated number, the dipole rotation time of associated FA,τ_{aFA}, was determined and the value of τ_{aFA} is higher than that of bulk FA, suggesting that the dynamics of associated FA is restricted by the hydrophilic chain of surfactant. Further analysis of thermodynamic parameters, obtained from the temperature dependences of the relaxation times, revealed that in dilute TX100−FA solution the interaction of FA with EO segment of surfactant is weaker than a FA−FA hydrogen bond.

The dynamic properties of hydration water in TX100−water mixtures were also determined in the same way. We found that although there are quantitative differences the dynamics of associated FA is quite similar to that of hydration water. This shows that the effect of interaction of hydrophilic chains on associated FA is similar to that on hydration water. This similarity of interaction may lead to similar micellization behaviors between surfactant−FA and surfactant−water systems.

This work provides some physical picture of the dynamics of associated FA. It may be noted that the results obtained are based on nonionic surfactant systems. Further studies on dynamics of associated FA in ionic surfactant systems are still ongoing.

■ ASSOCIATED CONTENT

Supporting Information

Detailed density measurement and calculation of partial volumes. This material is available free of charge via the Internet at http://pubs.acs.org.

■ AUTHOR INFORMATION

Corresponding Author

*Tel: +86010-58808283. E-mail: zhaoks@bnu.edu.cn.

Notes

The authors declare no competing financial interest.

■ ACKNOWLEDGMENTS

We thank Dr. S. J. Zhao of the School of Geography, Beijing Normal University for providing the laboratory facilities of high-frequency dielectric measurements. Financial support of this work by the National Natural Science Foundation of China (nos. 21173025 and 20976015) and the Major Research Plan of NSFC (21233003) are gratefully acknowledged.

■ REFERENCES

(1) Bleasdale, T. A.; Tiddy, G. J. T.; Wyn-Jones, E. Cubic Phase Formation In Polar Nonaqueous Solvents. *J. Phys. Chem.* **1991**, *95*, 5385−5386.

(2) Gamboa, C.; Ríos, H.; Sanchez, V. Surfactant Aggregation in Formamide. *Langmuir* **1994**, *10*, 2025−2027.

(3) Rico, I.; Lattes, A. Formamide, a Water Substitute. 12. Krafft Temperature and Micelle Formation of Ionic Surfactants in Formamide. *J. Phys. Chem.* **1986**, *90*, 5870−5872.

(4) Das, J.; Ismail, K. Aggregation, Adsorption, and Clouding Behaviors of Triton X-100 in Formamide. *J. Colloid Interface Sci.* **2009**, *337*, 227−233.

(5) Jonströmer, M.; Sjöberg, M.; Wärnheim, T. Aggregation and Solvent Interaction in Nonionic Surfactant Systems with Formamide. *J. Phy. Chem.* **1990**, *94*, 7549−7555.

(6) Alexandridis, P.; Yang, L. Micellization of Polyoxyalkylene Block Copolymers in Formamide. *Macromolecules* **2000**, *33*, 3382−3391.

(7) Alexandridis, P. Structural Polymorphism of Poly(ethylene oxide)-Poly(propylene oxide) Block Copolymers in Nonaqueous Polar Solvents. *Macromolecules* **1998**, *31*, 6935−6942.
(8) Kaatze, U.; Gottmann, O.; Podbielski, R.; Pottel, R.; Terveer, U. Dielectric Relaxation in Aqueous Solutions of Some Oxygen-Containing Linear Hydrocarbon Polymers. *J. Phys. Chem.* **1978**, *82*, 112−120.
(9) Bagchi, B. Water Dynamics in the Hydration Layer around Proteins and Micelles. *Chem. Rev.* **2005**, *105*, 3197−3219.
(10) Nandi, N.; Bhattacharyya, K.; Bagchi, B. Dielectric Relaxation and Solvation Dynamics of Water in Complex Chemical and Biological Systems. *Chem. Rev.* **2000**, *100*, 2013−2045.
(11) Jia, L. W.; Guo, C.; Yang, L. G.; et al. Mechanism of PEO-PPO-PEO Micellization in Aqueous Solutions Studied by Two-Dimensional Correlation FTIR Spectroscopy. *J. Colloid Interface Sci.* **2010**, *345*, 332−337.
(12) Kumbhakar, M.; Nath, S.; Mukherjee, T.; Pal, H. Solvation Dynamics in Triton X-100 and Triton X-165 Micelles: Effect of Micellar Size and Hydration. *J. Chem. Phys.* **2004**, *121*, 6026−6033.
(13) Beyer, K. Phase Structures, Water Binding, and Molecular Dynamics in Liquid Crystalline and Frozen States of the System Triton X-100-D_2O: A Deuteron and Carbon NMR Study. *J. Colloid Interface Sci.* **1982**, 86−73.
(14) Riter, R. E.; Undiks, E. P.; Kimmel, J. R.; Levinger, N. E. Formamide in Reverse Micelles: Restricted Environment Effects on Molecular Motion. *J. Phys. Chem. B* **1998**, *102*, 7931−7938.
(15) Shirota, H.; Segawa, H. Solvation Dynamics of Formamide and *N*,*N*-Dimethylformamide in Aerosol OT Reverse Micelles. *Langmuir* **2004**, *20*, 329−335.
(16) Corea, N. M.; Pires, P. A. R.; Silber, J. J.; El Seoud, O. A. Real Structure of Formamide Entrapped by AOT Nonaqueous Reverse Micelles: FT-IR and ^{1}H NMR Studies. *J. Phys. Chem. B* **2005**, *109*, 21209−21219.
(17) Lattes, A.; Perez, E.; Rico-Lattes, I. Organized Molecular Systems in Structured Non-aqueous Solvents. Is Formamide a Water Like Solvent? *C. R. Chim.* **2009**, *12*, 45−53.
(18) Gekle, S.; Netz, R. R. Anisotropy in the Dielectric Spectrum of Hydration Water and Its Relation to Water Dynamics. *J. Chem. Phys.* **2012**, *137*, 104704.
(19) Lusceac, S. A.; Gainaru, C.; Ratzke, D. A.; Graf, M. F.; Vogel, M. Secondary Water Relaxation in a Water/Dimethyl Sulfoxide Mixture Revealed by Deuteron Nuclear Magnetic Resonance and Dielectric Spectroscopy. *J. Phys. Chem. B.* **2011**, *115*, 11588−11596.
(20) Asami, K. Dielectric Properties of Water in Triton X-100 (nonionic detergent)-water Mixtures. *J. Phys.: Condens. Matter* **2007**, *19*, 37610.
(21) Baar, C.; Buchner, R.; Kunz, W. Dielectric Relaxation of Cationic Surfactants in Aqueous Solution. 2. Solute Relaxation. *J. Phys. Chem. B* **2001**, *105*, 2914−2922.
(22) Schrödle, S.; Hefter, G.; Kunz, W.; Buchner, R. Effects of Nonionic Surfactant $C_{12}E_5$ on the Cooperative Dynamics of Water. *Langmuir* **2006**, *22*, 924−932.
(23) Singh, L. P.; Cerveny, S.; Alegría, A.; Colmenero, J. Dynamics of Water in Supercooled Aqueous Solutions of Poly(propylene glycol) As Studied by Broadband Dielectric Spectroscopy and Low-Temperature FTIR-ATR Spectroscopy. *J. Phys. Chem. B* **2011**, *115*, 13817−13827.
(24) Cametti, C.; Marchetti, S.; Gambi, C. M. C.; Onori, G. Dielectric Relaxation Spectroscopy of Lysozyme Aqueous Solutions: Analysis of the δ-Dispersion and the Contribution of the Hydration Water. *J. Phys. Chem. B* **2011**, *115*, 7144−7153.
(25) Hanai, T.; Zhang, H. Z.; Sekine, K.; Asaka, K.; Asami, K. The Number of Interfaces and the Associated Dielectric Relaxations in Heterogeneous Systems. *Ferroelectrics* **1988**, *86*, 191.
(26) Schwan, H. P. In *Physical Techniques in Biological Research*; Nastuk, W. L., Ed.; Academic Press: New York, 1963; Vol. *6*, p 373.
(27) Bordi, F.; Cametti, C.; Biasio, A. D. Electrical Conductivity Behavior of Poly(ethylene oxide) in Aqueous Electrolyte Solutions. *J. Phys. Chem.* **1988**, *92*, 4772−4777.
(28) Lian, Y. W.; Zhao, K. S. Study of Micelles and Microemulsions Formed in a Hydrophobic Ionic Liquid by a Dielectric Spectroscopy Method. I. Interaction and Percolation. *Soft Matter* **2011**, *7*, 8828.
(29) Lian, Y. W.; Zhao, K. S. Dielectric Analysis of Micelles and Microemulsions Formed in a Hydrophilic Ionic Liquid. I. Interaction and Percolation. *J. Phys. Chem. B* **2011**, *115*, 11368−11374.
(30) Bordi, F.; Cametti, C.; Gili, T. Reduction of the Contribution of Electrode Polarization Effects in the Radiowave Dielectric Measurements of Highly Conductive Biological Cell Suspensions. *Bioelectrochemistry* **2001**, *54*, 53−61.
(31) Bruggeman, D. A. G. Berechnung Verschiedener Physikalischer Konstantenvon Heterogenen Substanzen. *Ann. Phys.* **1935**, *24*, 636.
(32) Looyenga, H. Dielectric Constants of Heterogeneous Mixtures. *Physica* **1965**, *31*, 401.
(33) Kurland, R. J.; Wilson, E. B. Microwave Spectrum, Structure, Dipole Moment, and Quadrupole Coupling Constants of Formamide. *J. Chem. Phys.* **1957**, *27*, 585−590.
(34) Pauling, L. *The Nature of the Chemical Bond*, 2nd ed.; Cornell University Press: Ithaca, 1948; p 133.
(35) Sato, T.; Hossain, Md. K.; Acharya, D. P.; Glatter, O.; Chiba, A.; Kunieda, H. Phase Behavior and Self-Organized Structures in Water/Poly(oxyethylene) Cholesteryl Ether Systems. *J. Phys. Chem. B* **2004**, *108*, 12927−12939.
(36) Sterpone, F.; Pierleoni, C.; Briganti, G.; Marchi, M. Molecular Dynamics Study of Temperature Dehydration of a $C_{12}E_6$ Spherical Micelle. *Langmuir* **2004**, *20*, 4311−4314.
(37) Hanai, T.; Imakita, A.; Koizumi, N. Systematic Analysis to Determine of Dielectric Phase Parameters from Dielectric Relaxations Caused by Diphasic Structure of Disperse Systems. *Bull. Inst. Chem. Res., Kyoto Univ.* **1977**, *55*, 4.
(38) Sengwa, R. J. Dielectric Behaviour and Relaxation in Poly(propylene glycol)-Water Mixtures Studied by Time Domain Reflectometry. *Polym. Int.* **2004**, *53*, 744−748.
(39) Shikata, T.; Takahashi, R.; Sakamoto, A. Hydration of Poly(ethylene oxide)s in Aqueous Solution as Studied by Dielectric Relaxation Measurements. *J. Phys. Chem. B* **2006**, *110*, 8941−8945.
(40) Borodin, O.; Bedrov, D.; Smith, G. D. Molecular Dynamics Simulation Study of Dielectric Relaxation in Aqueous Poly(ethylene oxide) Solutions. *Macromolecules* **2002**, *35*, 2410−2412.
(41) Shinyashiki, N.; Yagihara, S.; Arita, I.; Mashimo, S. Dynamics of Water in a Polymer Matrix Studied by a Microwave Dielectric Measurement. *J. Phys. Chem. B* **1998**, *102*, 3249−3251.
(42) Cole, K. S.; Cole, R. H. Dispersion and Absorption in Dielectrics. I. Alternating Current Characteristics. *J. Chem. Phys.* **1941**, *9*, 341.
(43) Cavell, E. A. S.; Knight, P. C.; Sheikh, M. A. Dielectric Relaxation in Non Aqueous Solutions. Part 2-Solutions of Tri(n-butyl) ammonium Picrate and Iodide in Polar Solvents. *J.Chem.Soc., Faraday Trans.* **1971**, *67*, 2225.
(44) Shinyashiki, N.; Matsumura, Y.; Miura, N.; Yagihara, S.; Mashimo, S. Dielectric Study of Water Structure in Polymer Solution. *J. Phys. Chem.* **1994**, *98*, 13612.
(45) Smith, G.; Shekunov, B. Y.; Shen, J.; Duffy, A. P.; Anwar, J.; Wakerly, M. G.; Chakrabari, R. Dielectric Analysis of Phosphorylcholine Head Group Mobility in Egg Lecithin Liposomes. *Pharm. Res.* **1996**, *13*, 1181−1185.
(46) Barthel, J.; Buchner, R.; Wurm, B. The Dynamics of Liquid Formamide, N-methylformamide, N,N-dimethylformamide, and N,N-dimethylacetamide. A Dielectric Relaxation Study. *J. Mol. Liq.* **2002**, *98−99*, 51−69.
(47) Buchner, R.; Barthel, J.; Stauber, J. The Dielectric Relaxation of Water between 0°C and 35°C. *Chem. Phys. Lett.* 306(1999)57.
(48) Frank, H. S.; Evans, M. W. Free Volume and Entropy in Condensed Systems III. Entropy in Binary Liquid Mixtures. *J. Chem. Phys.* **1945**, *13*, 507−532.